NIH RELAIS Document Delivery

NIH-10096742

NIH -- W1 MA34HM

PAMELA GEHRON ROBEY
CSDB/NIDR/NIH Bldng 30 Rm 228
30 CONVENT DRIVE MSC 4320
BETHESDA, MD 20892

ATTN:		SUBMITTED:	2001-12-21 15:25:39
PHONE:	301-496-4563	PRINTED:	2001-12-27 09:04:02
FAX:	301-402-0824	REQUEST NO.:	NIH-10096742
E-MAIL:		SENT VIA:	LOAN DOC
			5363448

NIH Fiche to Paper Journal

TITLE:	MAGNETIC RESONANCE IMAGING CLINICS OF NORTH AMERICA
PUBLISHER/PLACE:	Saunders Philadelphia Pa
VOLUME/ISSUE/PAGES:	1998 Aug;6(3):561-77 561-77
DATE:	1998
AUTHOR OF ARTICLE:	Meyer JS; Dormans JP
TITLE OF ARTICLE:	Differential diagnosis of pediatric musculoskeleta
ISSN:	1064-9689
OTHER NOS/LETTERS:	Library does NOT report holding title 9422762 9654585
SOURCE:	PubMed
CALL NUMBER:	W1 MA34HM
REQUESTER INFO:	AB424
DELIVERY:	E-mail: probey@DIR.NIDCR.NIH.GOV
REPLY:	Mail:

1064–9689/98 $8.00 + .00

DIFFERENTIAL DIAGNOSIS OF PEDIATRIC MUSCULOSKELETAL MASSES

James S. Meyer, MD, and John P. Dormans, MD

MR imaging plays a major role in the evaluation of children with soft-tissue and bone tumors. Although the imaging characteristics of these lesions are often nonspecific, MR imaging provides valuable information on the extent of disease and relationship of tumors to the neurovascular bundle and other vital structures. This article reviews the radiographic and MR imaging appearances and clinical presentations of a wide range of musculoskeletal masses that occur in children.

Children with bone and soft-tissue tumors usually present with pain or a focal mass. Plain radiographs usually are the first imaging study used to determine whether the abnormality is in the soft tissue or in bone. When a bone lesion is detected, the plain radiographic appearance helps determine the need for additional imaging. Some benign lesions require no further imaging or treatment, whereas for others CT or MR imaging is useful for developing a differential diagnosis and for preoperative planning. Malignant bone lesions are virtually always assessed with MR imaging.

When there is a soft-tissue mass without an underlying bone lesion, the need for further imaging depends on the history and physical examination. A soft-tissue mass that develops following trauma may be a hematoma that initially requires only close clinical follow-up, with imaging reserved for masses that persist or grow. When a cystic mass, such as a popliteal cyst, is suspected, ultrasound can be done for confirmation, although MR imaging is recommended if there is concern for internal joint derangement. In most other situations, MR is used to evaluate soft-tissue tumors.

PROTOCOLS

Different MR imaging protocols are used to evaluate soft-tissue masses, benign-appearing bone lesions, or malignant-appearing bone lesions. There are, however, a few principles that should be applied to the MR imaging of all children with musculoskeletal tumors.

To supplement information provided by the referring physician, available radiographs of the area of interest are reviewed, a brief history is obtained from the parent (or patient), and the patient is examined. When there is a soft-tissue mass, vitamin E capsules are placed on the overlying skin to mark the area of interest. The patient's ability to cooperate is assessed and sedation or pain medication is administered according to an approved protocol[21] with emergency personnel and equipment readily available. If the patient will require gadolinium injection during the examination, intravenous access is established prior to sedation.

After reviewing the plain radiographs, MR coil(s) are chosen for the examination. The goals are to obtain high-resolution images and cover the entire area of interest. The examination, however, needs to be performed in a timely manner, especially in a sedated child or a child experiencing significant pain. Optimally, the smallest coil that will allow for adequate coverage is used.

When the area of interest is on the trunk, the head coil is used for small patients and either the body coil or a phased-array body coil is used for large patients. Extremity tumors may require multiple

From the Departments of Radiology (JSM) and Orthopedic Surgery (JPD), University of Pennsylvania School of Medicine; and The Children's Hospital of Philadelphia (JSM, JPD), Philadelphia, Pennsylvania

coils. For instance, in a small child with an extensive thigh lesion, a phased array coil is used that can be repositioned to cover the entire lesion or involved bone is used. In a large child, a surface coil is used for high-resolution axial imaging of the tumor and the body coil is used for long axis views of the entire bone. Sometimes, the body coil alone provides adequate quality for imaging an extensive abnormality in a large child.

MR imaging examinations should be tailored to obtain specific information. The following protocols are recommended to evaluate children with bone and soft-tissue tumors.

Soft-Tissue Tumor Protocol

In children with soft-tissue tumors, MR imaging is done mainly to better determine the size and location of the tumor and its relationship to other structures, including the neurovascular bundle. This information, in conjunction with the history, clinical examination, and the lesion's intrinsic MR imaging characteristics enable the development of a differential diagnosis and a surgical plan.

Axial T1-weighted, T2-weighted, and gradient-echo sequences are done through the tumor. When the lesion is near a joint, a long axis scan is done using whichever sequence best delineated the tumor. Additional T1-weighted sequences (usually with fat saturation) are performed if gadolinium is administered.

T2-weighted images usually delineate lesion extent. T1-weighted images supplement this information, especially in lesions with fibrous and fatty components, and are useful for tumor characterization. The gradient-echo sequences define neurovascular bundle location, determine the presence of large or high-flow vessels in the tumor, and confirm the presence of hemorrhagic products in the tumor. The postgadolinium sequences determine the presence of cystic or necrotic components, differentiate joint fluid from synovial hypertrophy or mass, and distinguish venous from lymphatic components in slow-flow vascular malformations.

Benign Bone Tumor Protocol

MR imaging is performed in children with benign-appearing bone tumors when it is necessary to determine the extent of tumor in the medullary cavity, confirm the absence of an associated soft-tissue mass, or delineate the relationship of the tumor to the neurovascular bundle and other important structures.

Evaluation of these tumors includes axial T1-weighted and T2-weighted sequences and a long axis scan, often using gradient-echo sequences. Axial gradient-echo sequences are done when the location of the neurovascular bundle is an issue.

The degree of medullary involvement is defined on the T1-weighted and T2-weighted sequences and any suspicion of a soft-tissue mass is well evaluated with these sequences. The combination of long- and short-axis images delineates lobulation or septation in cystic lesions. The T2-weighted sequences are quite sensitive to the presence of fluid-fluid levels.

Malignant Bone Tumor Protocol

In children with malignant-appearing bone tumors, MR imaging assesses tumor extent, size, and relationship to the neurovascular bundle and other structures such as the physis, joint, and muscle compartments. MR imaging has less of a role in the differential diagnosis because virtually all of these lesions will undergo biopsy. MR imaging, however, is helpful for planning the initial biopsy and crucial to determine if the patient is a candidate for limb-sparing surgery.

Axial T1-weighted and T2-weighted and long axis T1-weighted sequences are done through the entirety of the involved bone and axial gradient echo sequences through the area of tumor. Small field of view, long axis scans, usually as T2-weighted sequences are used to evaluate joint involvement. Long axis STIR sequences and postgadolinium imaging are optional.

The entire involved bone is imaged to look for skip lesions. The images from axial T2-weighted sequences, especially the proton density-weighted images, usually define the soft-tissue portion of the tumor. These images together with axial gradient-echo sequences show the relationship of the tumor to the neurovascular bundle. T1-weighted images are reviewed together with the T2-weighted axial images to assess lesion extent. The high-resolution, long-axis, T2-weighted images are helpful to detect a joint effusion or extension of tumor into the joint. Short term inversion-recovery (STIR) sequences are helpful for confirmation of inconclusive findings seen on other sequences. Postgadolinium imaging can distinguish tumor from edema[30] and determine the amount of tumor necrosis.

DIFFERENTIAL DIAGNOSIS OF BONE TUMORS

The plain radiograph is the most useful imaging study to determine the differential diagnosis of a bone lesion. Radiographs should be reviewed with attention to the margin, associated periosteal reaction, matrix, and location of a lesion. This information can help estimate lesion aggressiveness, and, in conjunction with the patient's age, can be used to develop and limit a differential diagnosis. The MR imaging correlates to these plain radiographic characteristics reflect interesting physiologic aspects of disease and MR imaging findings occasionally offer further insight into the diagnostic possibilities.

Margins

On plain radiographs, the bone tumor margin is the result of the balance between bone destruction by host osteoclasts in response to the tumor and adjacent osteoblastic activity. The perception of bone destruction depends on both the degree of bone loss and the amount of adjacent bone available for contrast. Generally, lesions in the well-trabeculated metaphysis are more easily seen than those in the diaphysis. Slow-growing tumors are usually benign and appear as well-defined lesions with geographic (Fig. 1*A*) and often sclerotic (Fig. 1*B*) margins. Faster growing tumors are often malignant and appear as poorly defined lesions with moth-eaten or permeative pattern and indistinct margins (see Fig. 1*C*).[33]

The bone tumor margin on MR imaging primarily reflects the amount of perilesional inflammation.[22] As a result, benign lesions such as infections, osteoid osteoma (Fig. 2*A*), chondroblastoma, and Langerhans cell histiocytosis (LCH) that elicit an inflammatory response can have indistinct margins.[22] Other benign lesions and many malignant lesions have sharply defined margins (see Fig. 2*B*). Different MR imaging sequences, however, may provide conflicting information about the tumor margin and extent of malignant disease in the bone.

Distinguishing between bone marrow edema and tumor can be difficult. Dynamic postcontrast MR imaging can help differentiate them,[30] but requires additional software and postprocessing and is not in general use. Both tumor and bone marrow edema have abnormal signal intensity (low on T1 weighting, high on T2 weighting, high on STIR). Because it is crucial in children with musculoskeletal sarcomas that all of the primary tumor be resected and that wide surgical margins be used, a conservative approach is best. All low T1 or high T2 weighting signal intensity in the bone is considered abnormal and presumed to represent tumor. Similarly, although STIR sequences are known to overestimate tumor extent,[47] abnormal STIR signal is best considered to represent tumor when it occurs in areas that are questionable on other sequences. When signal abnormalities suggest a skip lesion that will significantly alter the child's surgical management, however, that area is biopsied prior to definitive surgery.

Periosteal Reaction

Periosteal reaction on radiographs may be positive, adding bone to the cortex, or negative, removing bone from the cortex. The positive periosteal reaction seen in association with a bone tumor reflects the amount of periosteal new bone produc-

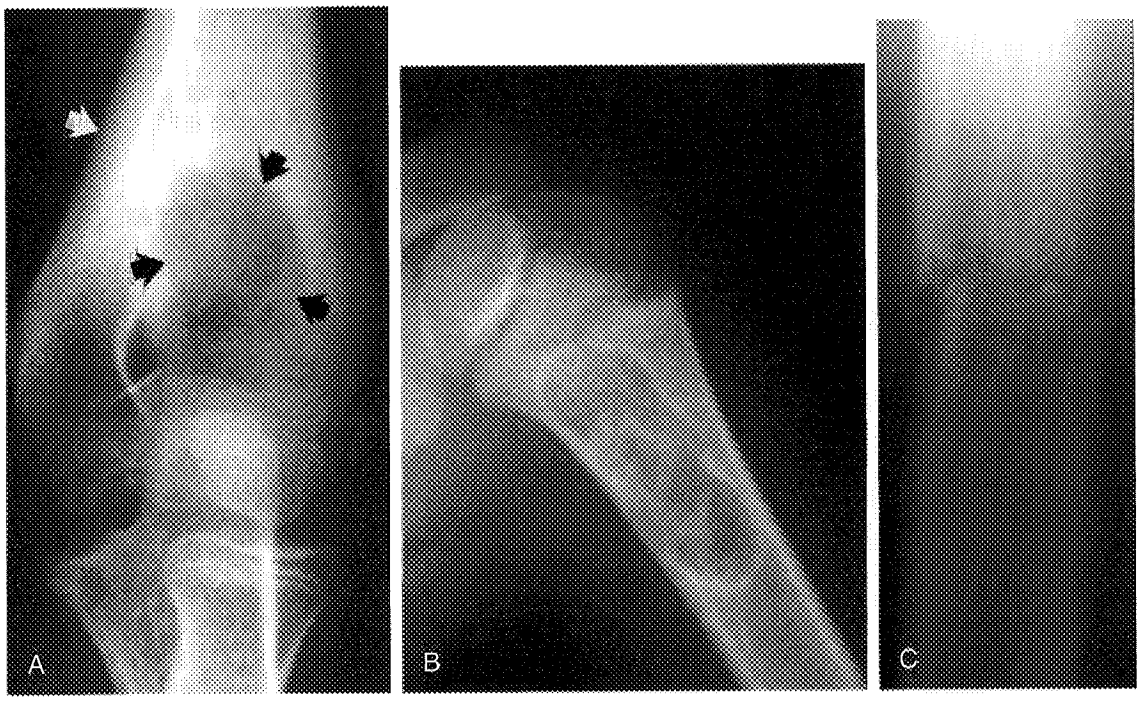

Figure 1. Tumor margins on plain radiographs. *A*, Osteoblastoma (*black arrows*) of the distal humerus has a well-defined but nonsclerotic margin. Dense periosteal new bone (*white arrow*) also is present. *B*, Nonossifying fibroma in proximal humerus has a sharply defined and sclerotic margin. *C*, Ewing sarcoma in femoral diaphysis has permeative pattern with indistinct margins. There is a pathologic fracture and lamellated periosteal new bone is present.

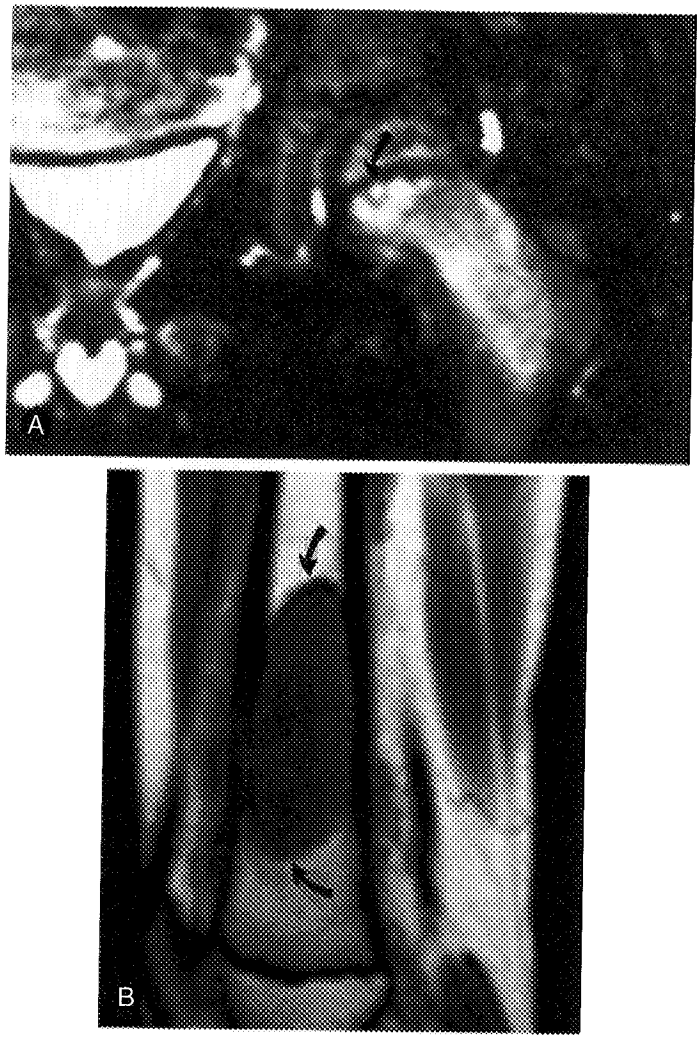

Figure 2. Tumor margins on MR images. *A*, Coronal T2-weighted image of osteoid osteoma shows high signal intensity with poorly defined margins involving femoral neck and proximal metaphysis. Center of nidus has high signal intensity (*arrow*) with a rim of low signal intensity. *B*, Sagittal T1-weighted image shows sharply defined margins (*arrows*) in osteosarcoma of the distal femur.

tion, degree of periosteal elevation, and activity of the tumor stimulating its production. Periosteal reaction must be mineralized to be visible on plain radiographs. There are three basic plain film appearances for positive periosteal reaction: (1) continuous; (2) interrupted; and (3) combined.[51]

Continuous periosteal reaction can result in a variety of appearances. In slow-growing processes such as bone cysts, endosteal resorption occurs in conjunction with periosteal apposition and gives the bone an expanded, shell-like appearance. Other types of continuous periosteal reaction lead to thickening of the bony cortex. This continuous reaction may be solid (see Fig. 1*A*), lamellated (Fig. 3*A*), or spiculated, with each of these types representing a progressively more aggressive lesion. Interrupted periosteal reactions (Fig. 3*B*) often reflect tumor growth exceeding the capacity of the elevated periosteum to lay down bone. They also can represent tumor breaking through the periosteum or resorption of previously present periosteal new bone. Periosteal interruption is generally, but not always, due to malignant disease. Combined reactions may represent a mixed pattern occurring in a single lesion, but also can occur when a chronic lesion becomes more active or following a fracture.[51]

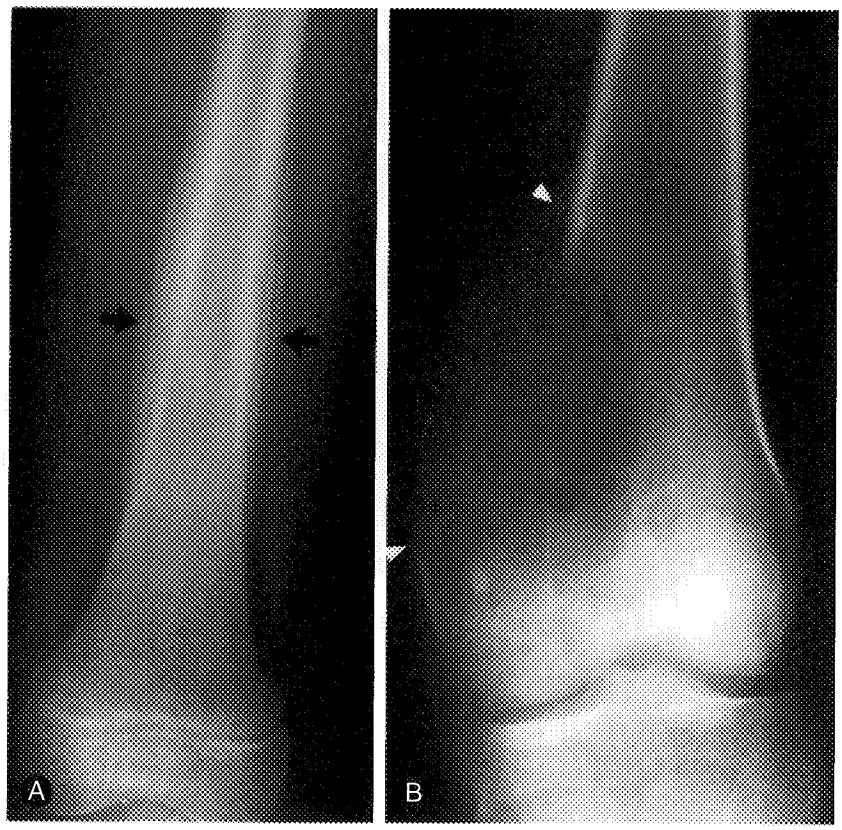

Figure 3. Periosteal reaction on plain radiographs. *A*, Lamellated periosteal reaction (*arrows*) is seen along the distal diametaphysis of the femur in a child with osteosarcoma. *B*, Codman's triangles (*arrowheads*) resulting from soft-tissue mass breaking through cortex and mineralized periosteum are present in the distal femoral metaphysis in another child with an osteosarcoma.

On MR imaging, the periosteum has low signal intensity on all imaging sequences and periosteal elevation is detectable even when the periosteum is not mineralized.[22] The MR appearance of mineralized periosteal reaction reflects degree and maturity of mineralization and the presence of intermingled soft tissue. Mature, solid mineralized periosteum is of low signal intensity on all sequences. Thin, shell-like periosteum may be only barely perceptible. Lamellated reaction contains areas of high signal intensity soft tissue alternating with areas of calcified periosteum (Fig. 4).

MR imaging is more sensitive to soft-tissue tumor extension than plain radiography. Soft-tissue extension suggests malignant disease, but also can be seen in benign diseases such as infection, LCH, giant cell tumor,[32] and fibrous dysplasia.[66]

Matrix

The internal appearance of the tumor depends on a combination of the tumor cells and matrix. Tumor matrix is the substance produced by the tumor cells. Some tumors (Ewing's sarcoma, bone cyst) do not produce matrix. Other tumors produce matrix that is either osteoid, chondroid, fibrous, myxoid, or a combination of these materials. Like periosteum, unless it is mineralized, tumor matrix will not be apparent on plain radiographs.[59]

The plain radiographic appearance of mineralized matrix has diagnostic significance. Mineralized osteoid matrix appears as homogeneous areas of opacity on plain radiographs. Mineralized chondroid matrix has a stippled, flocculent, or solid pattern. A pattern of calcified rings and arcs can develop around cartilage lobules.[59]

On MR imaging, benign and malignant bone tumors have predominantly low signal intensity on T1-weighted sequences and intermediate to high signal intensity on T2-weighted sequences. The degree of matrix calcification, however, greatly influences this appearance and areas of calcification or septation can result in low signal intensity foci on all sequences. Gadolinium enhancement reflects lesion

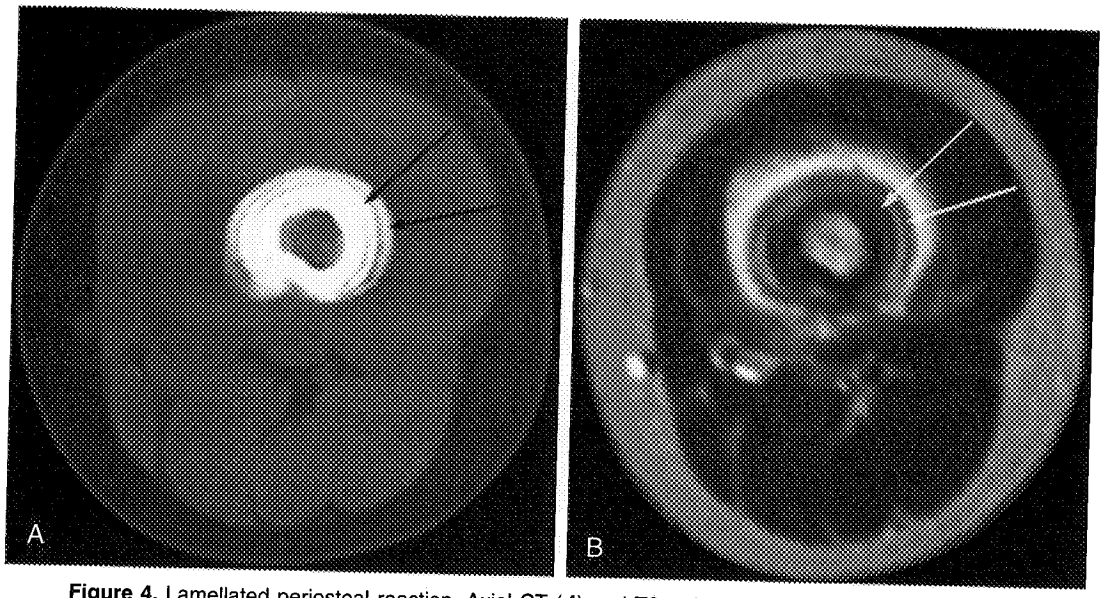

Figure 4. Lamellated periosteal reaction. Axial CT (*A*) and T2-weighted image (*B*) at corresponding level show mineralized periosteum (*arrows*) alternating with soft tissue.

vascularity and can be seen to varying degrees in both malignant and benign tumors.[63] Tumors of fibrous and cartilaginous matrix, when not mineralized, tend to have intermediate to high signal intensity on T2-weighted sequences. Uncomplicated bone cysts usually contain high signal intensity fluid on T2-weighted sequences. Occasionally a fluid-fluid level (Fig. 5) caused by hemorrhage is seen in a bone tumor. This was originally described in an aneurysmal bone cyst (ABC)[5] but has since been seen in a variety of bone tumors including chondroblastoma, giant cell tumor, fibrous dysplasia, simple bone cyst, malignant fibrous histiocytoma, and osteosarcoma.[61]

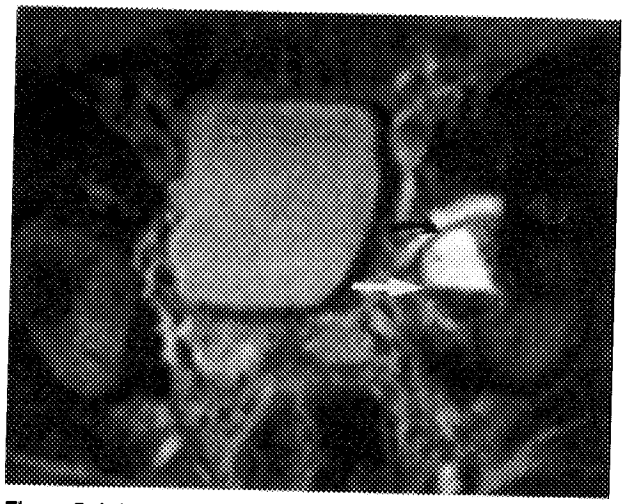

Figure 5. Axial T2-weighted image shows a fluid-fluid level (*arrow*) due to blood in an aneurysmal bone cyst of the pubic bone. There is thin, shell-like periosteal reaction that was barely perceptible on plain radiography, but is seen as a black line (*curved arrow*) between tumor and surrounding soft-tissue edema.

Selected Benign Bone Tumors

Bone Cysts

Simple and aneurysmal bone cysts are relatively common lesions in children and more than 85% occur in patients less than 20 years of age. Simple bone cysts are fluid-filled tumors that are lined by fibrous tissue and a single row of mesothelial-like cells. Most are centrally located in the medullary cavity. They are usually metaphyseal, but may be seen in the diaphysis and rarely cross the physis to involve the epiphysis. Sixty-two percent of simple bone cysts involve the proximal humerus and 27% the proximal femur.[36]

Aneurysmal bone cysts have cyst-like walls of predominantly fibrous tissue filled with free-flowing blood. Aneurysmal bone cysts can be centrally or eccentrically located in the bone. Most occur in the long bones (53%) and spine (15%). Those occurring in the long bones tend to involve the metaphyses and those in the spine usually involve the posterior elements.[36]

A simple bone cyst often can be differentiated from an ABC by plain radiographic findings. When plain film findings are atypical, however, MR imaging often can suggest the correct diagnosis. The typical simple bone cyst is a single smoothly marginated lesion that contains homogeneous fluid with intermediate signal intensity on T1-weighted sequences and high signal intensity on T2-weighted sequences. ABCs often have internal septations and contain hemorrhagic material with fluid-fluid levels. Although there can be overlap in the appearance of bone cysts, if a cystic lesion has internal septations and hemorrhagic products, it is more likely an aneurysmal bone cyst than a simple cyst (R. J. Sullivan, MD, personal communication, 1995).

Osteochondroma

An osteochondroma is a benign, cartilage-capped lesion that grows out of the bone and typically points away from the adjacent joint. These tumors can affect virtually any bone with an epiphysis or apophysis and about 80% arise from the long bones.[39] These lesions are most often metaphyseal, but may occur in the diaphysis in older patients. Plain radiographic findings are characteristic. MR imaging is occasionally done in symptomatic patients[25, 62] and for surgical planning.

The continuity of the bone marrow and cortex of the osteochondroma with native bone (Fig. 6) and the relationship of the tumor to adjacent neurovascular structures are well-demonstrated with MR imaging.[25] Furthermore, MR imaging can show the cartilaginous cap, which should be considered suspicious for chondrosarcomatous transformation when it exceeds 2 cm in thickness in a skeletally mature patient.[39]

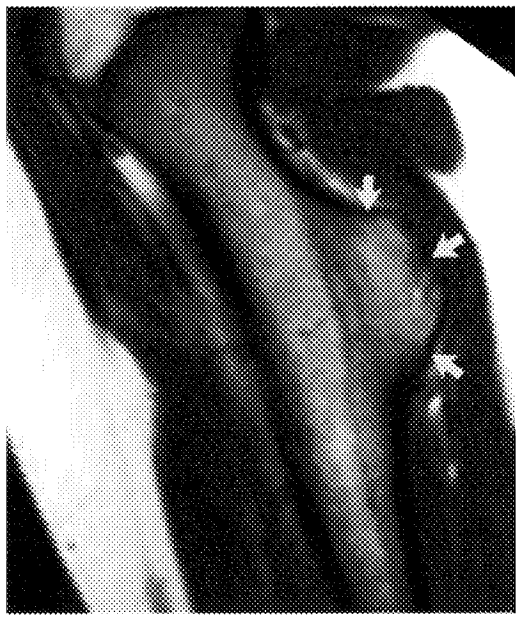

Figure 6. Long axis T1-weighted image shows continuity of native medullary cavity and cortical bone of the proximal humerus with an osteochondroma (*arrows*) in a 7-year-old boy. MR imaging was performed to define the relationship of the tumor to the neurovascular bundle.

Chondroblastoma

Chondroblastomas are benign cartilaginous tumors arising in the epiphyses and apophyses. Seventy percent of lesions are seen during active physeal growth and most occur in children between 10 and 20 years of age. Proximal humeral (18%), proximal tibial (17%), distal femoral (16%), and proximal femoral (12%) epiphyses are the most common sites of involvement. Lesions may extend to the metaphysis, but pure metaphyseal involvement is rare. On plain radiographs, lesions are oval to round with well-defined borders, many have a thin rim of sclerosis, and about half contain punctate opacities representing a calcification of cartilaginous matrix.[37] Periosteal reaction can occur adjacent or distant to the lesion.[64] The differential diagnosis for these lesions usually includes subacute osteomyelitis (Brodie's abscess) of the epiphysis.

On MR imaging, tumor margins often are lobular[64] but the internal signal characteristics vary.[48, 64, 65] The inflammatory nature of these tumors is reflected by bone marrow and soft-tissue edema and periosteal reaction.[48, 64, 65] The presence of these findings may be helpful for evaluation of patients with possible recurrence. In a group of four patients with clinically suspected recurrence, peritumoral bone marrow edema was present in one patient with recurrence and absent in three without recurrence.[48]

Osteoid Osteoma

Osteoid osteomas are often seen in adolescents and have a classic clinical presentation of pain that is most intense at night and relieved by aspirin; rarely, these lesions are painless. The nidus is osteoid rich and highly vascular in early lesions, whereas more mature lesions are less vascular. The lesion usually is close to the cortex and more than 80% occur in the long bones. Plain radiographs usually show a less than 2 cm area of abnormal bone that is lucent to extremely dense and associated with dense periosteal new bone. About 6% occur in the spine, in which they typically involve the posterior elements, near the pedicles.[40]

On MR imaging, the nidus (see Fig. 2*A*) may have low or intermediate signal intensity on T1-weighted sequences and low, intermediate, or high signal intensity on T2-weighted sequences.[4] When present, associated cortical new bone is of low intensity on all imaging sequences. The nidus enhanced variably following gadolinium administration.[67] The nidus, however, is not always well seen and MR imaging often shows signal abnormalities in the medullary bone and soft tissues that overestimate disease extent. For these reasons, CT is preferred when there is a strong clinical suspicion for osteoid osteoma.

Fibrous Dysplasia

Fibrous dysplasia is caused by a hamartomatous or tumor-like proliferation of fibroosseous tissue. Seventy-five percent of patients are less than 30 years of age at presentation. Lesions usually are monostotic and most involve the femur (36%), tibia (19%), and skull (17%).[40] Polyostotic disease can be associated with McCune-Albright syndrome, which often is manifest by the triad of bone lesions, cutaneous pigmentation (café-au-lait spots), and precocious puberty in girls.[2]

Fibrous dysplasia involves the medullary cavity and may result in bony expansion. A *ground-glass* appearance often is seen on plain radiographs and involvement of the proximal femur may result in a typical *shepherd's crook deformity.*[40]

MR imaging depicts medullary cavity involvement well. The signal characteristics of fibrous dysplasia vary (Fig. 7). Some areas have low signal intensity on T1- and T2-weighted sequences and others have high signal intensity on T2-weighted sequences.[13] Fibrous dysplasia may cause cortical thinning and areas of full-thickness cortical destruction as well as associated soft-tissue masses that can be seen on MR imaging.[66]

Osteofibrous Dysplasia

Osteofibrous dysplasia (also known as *Campanacci's disease* and *ossifying fibroma*) is a fibroosseous lesion that originates in the cortex and may extend into the medullary cavity of the tibia or fibula. These lesions typically begin in the anterior cortex of the bone, are oriented longitudinally, and cause cortex

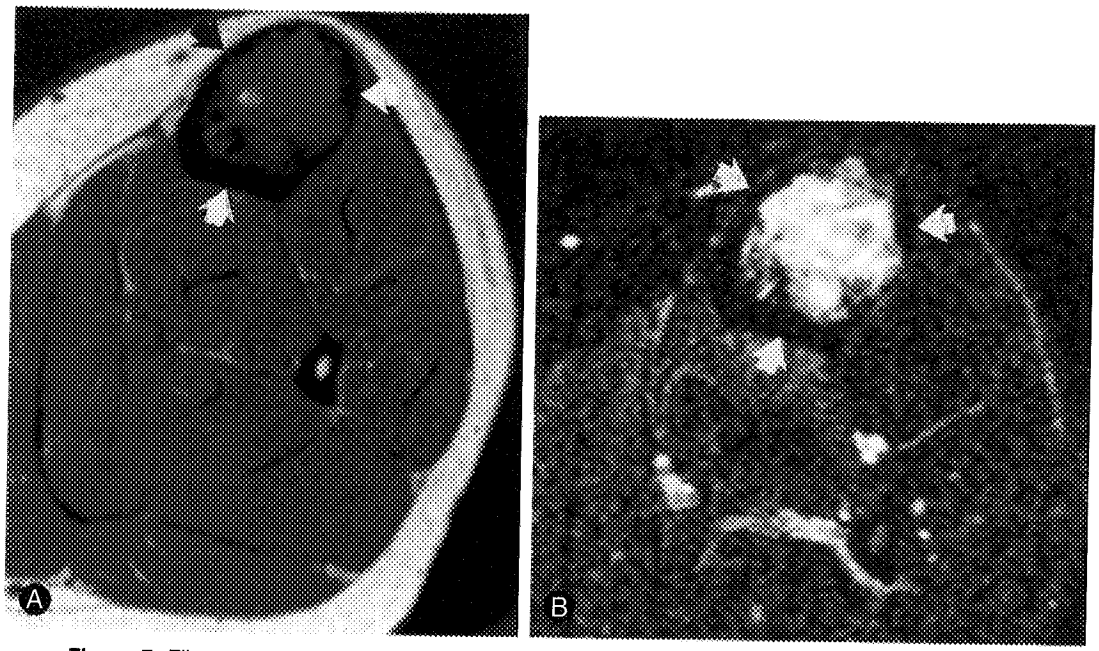

Figure 7. Fibrous dysplasia. *A*, Axial T1-weighted image shows predominantly low signal intensity material (*arrows*) filling the medullary cavity. *B*, This material has predominantly high signal intensity (*arrows*) on the corresponding T2-weighted image.

expansion. On plain radiographs, they have a lytic to *ground-glass* appearance with small to large lobular loculations and blastic to sclerotic margins. Some patients have anterior bowing deformity and pathologic fractures may occur. These lesions must be distinguished from fibrous dysplasia and adamantinoma, a rare low-grade malignancy that has a propensity to involve the anterior portion of the tibial and fibular diaphyses.[35]

The MR imaging signal characteristics of osteofibrous dysplasia are similar to those of fibrous dysplasia. MR imaging can help differentiate these lesions by demonstrating the cortical location of osteofibrous dysplasia and the medullary location of fibrous dysplasia.[13] Differentiating osteofibrous dysplasia from adamantinoma is more difficult and definitive diagnosis requires biopsy.

Biopsy is recommended if there is extraosseous extension of tumor, a permeative pattern on plain radiographs, or in patients seeking care after 20 years of age.[56] MR imaging can determine the presence of a soft-tissue mass,[14] prompting biopsy, and can demonstrate the cortical[68] and, when present, medullary extent of the lesion.

Selected Malignant Bone Tumors

Osteosarcoma

Osteosarcoma is a malignant tumor that produces osteoid and bone.[40] It is the most common malignant bone tumor in children.[19] Osteosarcomas may be high or low grade and intramedullary, intracortical, or juxtacortical in origin.[40]

The intramedullary, high-grade variant (classic osteosarcoma) comprises 75% of osteosarcomas.[40] Approximately 15% of children with these tumors present with metastatic lesions, usually to the lungs.[19] The primary tumor occurs most frequently in the distal femur (35%), proximal tibia (17%), and proximal humerus (10%). Ninety percent are located in the metaphysis, 9% are diaphyseal, and 1% occur in the epiphysis. These osteosarcomas are typically large (> 6 cm) with fluffy bone production, Codman's triangles, aggressive periosteal reaction, and a soft-tissue mass on plain radiographs. Less commonly, osteosarcomas, especially the telangiectatic variant, are purely lytic. Tumors developing in the diaphysis may have onion-skin periosteal new bone, stimulating a Ewing's sarcoma.[40]

These tumors typically show low signal intensity on T1-weighted images and heterogeneous high signal intensity on T2-weighted images in the medullary cavity and an associated soft-tissue mass (Fig. 8*A*). As would be expected, the more densely calcified tumors have more areas of low signal intensity on all imaging sequences. MR imaging is accurate in determining transphyseal spread of tumor into the epiphysis (see Fig. 8*B*)[49, 54] and very sensitive for detection of intraarticular involvement. MR imaging, however, is not very specific for joint involvement and peritumorous inflammatory changes may

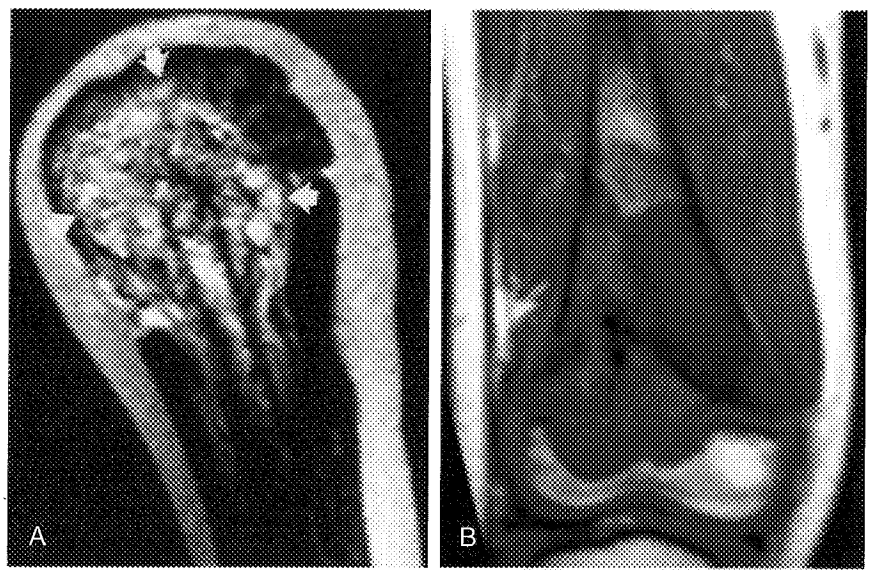

Figure 8. Osteosarcoma. *A*, Sagittal T2-weighted image shows large soft-tissue mass (*arrows*) of an osteosarcoma in the proximal humerus of an 11-year-old boy. *B*, Coronal T1-weighted image shows low signal intensity tumor crossing the physis into the distal femoral epiphysis in a 5-year-old boy.

cause false-positive diagnoses that can lead to unnecessarily radical surgery.[54]

Other, less common types of osteosarcoma are the periosteal and parosteal variants. Periosteal osteosarcoma is a low- to moderate-grade tumor that is extremely rare. Most of these tumors are diaphyseal and involve the tibia (51%) or femur (35%). This tumor has been seen in patients 9 to 70 years of age, but most patients are in their third decade. These tumors are saucer-shaped to fusiform, eccentric, juxtacortical masses and more than 50% display perpendicularly oriented bony spicules radiating from the cortex to the outer edge of the tumor.[39]

The parosteal variant may be low or high grade.[23] Parosteal osteosarcomas typically develop in the long bones, especially the distal femur of adults.[23] On plain radiographs, these densely calcified lesions may have a lucent noncalcified cleavage plane between the tumor and the cortex.[39] Most low-grade lesions have low signal intensity on T1- and T2-weighted sequences, whereas most tumors with high signal intensity on T2 weighting are high grade. MR imaging also can demonstrate the presence of marrow involvement (Fig. 9), which does not indicate a high-grade tumor, but should be completely excised to improve patient prognosis.[23]

Ewing's Sarcoma

Ewing's sarcoma is a highly malignant, round cell tumor of uncertain origin. It is the second most common malignant bone tumor in children. Twenty-five percent of children present with overt metastases, usually to the lungs, bone marrow, or bone.[19] Ewing's sarcoma can occur in any bone, but is most common in the femur (25%), ilium (14%), tibia (11%), and humerus (10%). Long bone involvement is described classically as middiaphyseal (33%), but metadiaphyseal (44%) involvement is actually more common and pure metaphyseal (15%) involvement can occur as well.[41]

On plain radiographs, Ewing's sarcoma may be lytic, mixed lytic-blastic, or predominantly sclerosis. Periosteal reaction may be *onion-skinning*, a single continuous line, or perpendicular striations (*hair on end*). Codman's triangles may be present.[41] In addition, cortical saucerization may occur.[44]

MR imaging characteristics are similarly varied (Fig. 10). In a review of 18 patients with Ewing's sarcoma that were lytic on plain radiographs, the involved portion of the medullary cavity had low signal intensity on T1-weighted sequences and there were associated soft-tissue masses in all patients. Sixteen tumors were isointense to fat on T2-weighted sequences. There was massive muscle edema in three tumors, but muscle edema was absent in eight.[16]

Lymphoma

Primary bone lymphoma is rare in children and some children who appear to have this tumor develop leukemia within 6 months of presentation. The femur (24%), ilium (17%), humerus (11%), and tibia (9%) are the most common sites of involvement, but lymphoma may occur in any bone. Le-

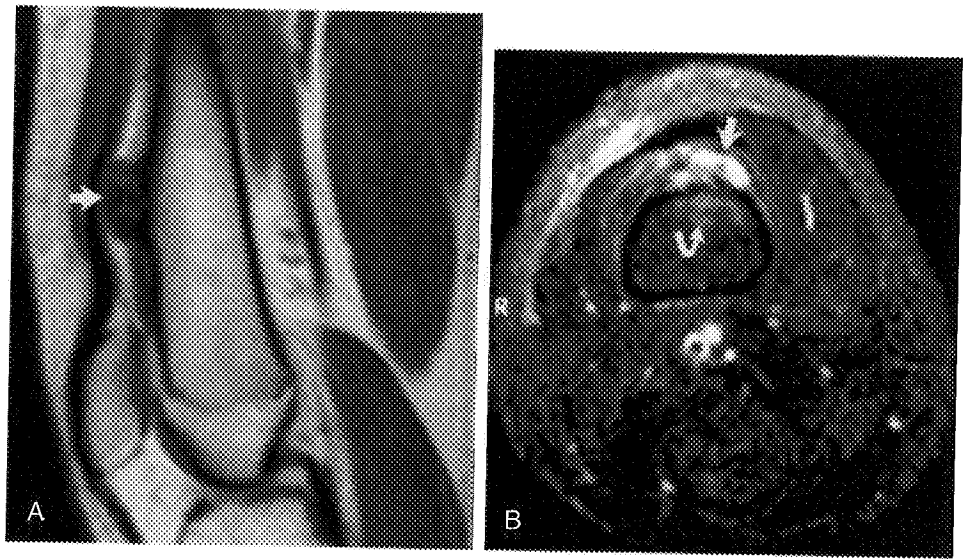

Figure 9. Parosteal osteosarcoma. *A*, Sagittal T1-weighted image shows mixed low and intermediate signal intensity tumor (*arrow*) adjacent to the anterior cortex of the distal femur. *B*, Axial T2-weighted image shows mixed intermediate and high signal intensity in tumor (*arrow*). High signal intensity seen in the medullary cavity (*curved arrow*) also was found to represent tumor.

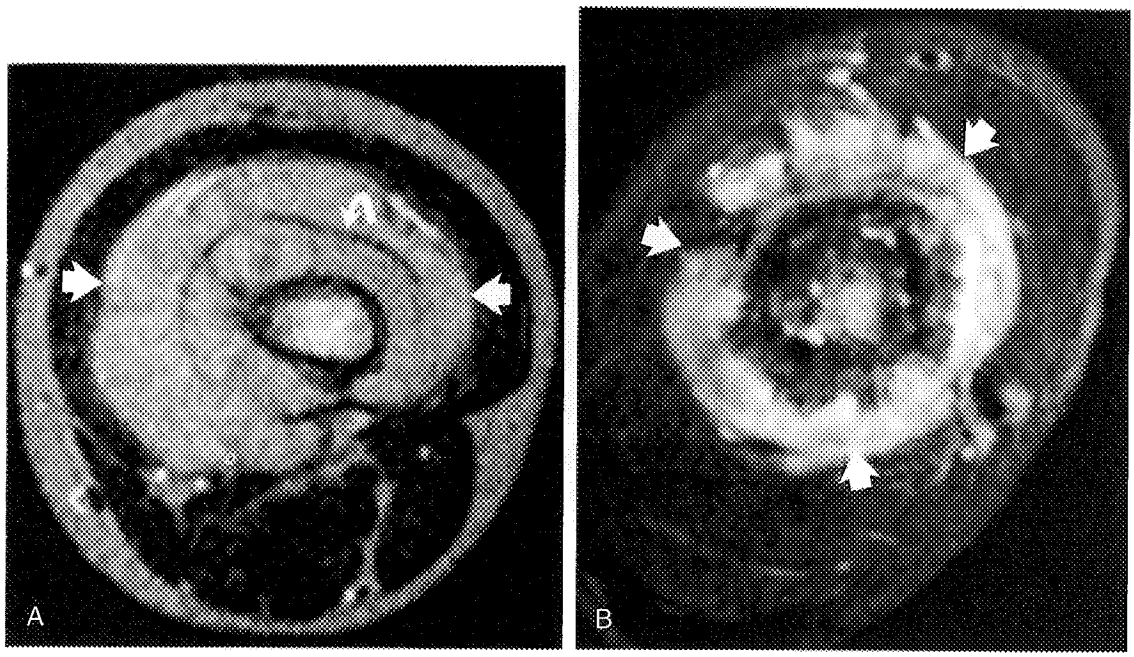

Figure 10. Ewing's sarcoma. *A*, Axial T2-weighted image shows large soft-tissue mass (*arrows*) surrounding the distal femur in a 4-year-old girl. Note the low signal intensity of the periosteum (*curved arrow*). *B*, Axial T2-weighted image with fat saturation shows high signal intensity in the medullary cavity and periphery (*arrows*), but predominantly low signal intensity in the remainder of the humerus in this 11-year-old boy. This tumor was densely sclerotic on plain radiography.

sions usually occur in the metaphysis or diaphysis and have an ill-defined, mixed lytic and blastic appearance on plain radiographs. Most other lesions are purely lytic; purely blastic lesions are very rare. There may be extensive permeative destruction, and periosteal reaction may be minimal or extensive. In addition, a soft-tissue mass can be present.[38]

MR imaging may show a medullary lesion or extensive intraosseous and extraosseous tumor. Interestingly, in one review[18] of primary bone lymphoma in four adults, MR imaging showed linear foci of abnormal signal intensity penetrating the cortex (Fig. 11). This suggests a mechanism whereby tumor can gain access to surrounding tissue without obvious cortical destruction.[18]

DIFFERENTIAL DIAGNOSIS OF SOFT-TISSUE TUMORS

Soft-tissue masses in children usually are benign.[7] History and clinical examination guide the evaluation of a soft-tissue mass, but biopsy often is necessary for histologic diagnosis. MR imaging is useful to confirm the presence of a mass and determine tumor size and location.

MR imaging characteristics are nonspecific and usually cannot predict histology. Well-defined margins and homogeneous internal signal intensities are seen on MR imaging in malignant and benign soft-tissue masses.[32] Similarly, both malignant and benign lesions can have ill-defined margins and heterogeneous internal signal intensity. Imaging following gadolinium administration can define necrotic and cystic areas, but has not been shown to significantly improve the differentiation of benign from malignant tumors.[7] Sometimes, however, MR imaging characteristics, especially in conjunction with the history and physical examination, allow an accurate diagnosis, as in patients with lipomas[32] and vascular malformations.

Selected Benign Soft-Tissue Tumors

Fatty Tumors

There are a wide variety of fatty tumors and most are more common in adults than in children. Simple lipomas are well-circumscribed, benign tumors composed of mature adipose tissue that typically are seen in adults in their fifth and sixth decades. Other benign variants of lipomas include lipomatosis and infiltrating lipomas, in which mature adipose tissue infiltrates through the soft tissues of the trunk or an extremity.[29] Lipoblastomas are immature lipomas

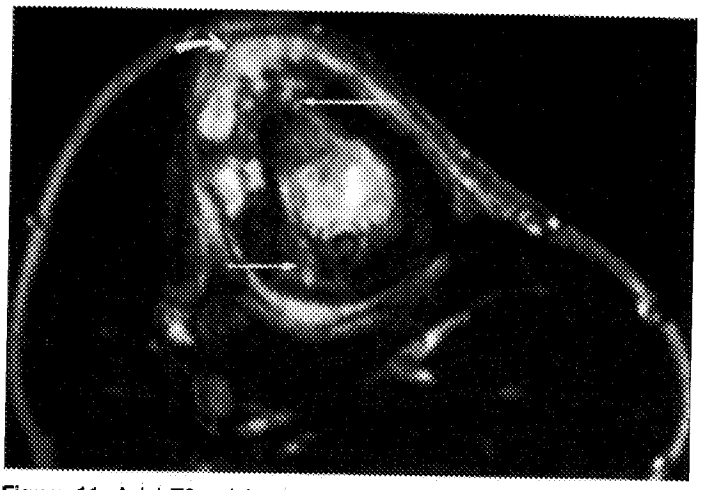

Figure 11. Axial T2-weighted image shows linear areas of high signal intensity (*long arrows*) extending through the cortex and soft-tissue mass (*curved arrow*) in this 16-year-old boy with primary lymphoma of the bone.

that occur almost exclusively in young children less than 3 years of age.[8] Two-thirds of these tumors are well circumscribed.[29] Those that infiltrate the muscles and subcutaneous tissues are referred to as *diffuse lipoblastomatosis*.[29] Liposarcomas are rare malignant tumors in children. When they occur in children, however, these tumors most often are found in the extremities and retroperitoneum.[42]

There is marked overlap in the MR imaging characteristics of these fatty tumors. Simple lipomas are well-circumscribed lesions with signal characteristics that approximate the subcutaneous fat on all imaging sequences. Lipoblastomas[26] and liposarcomas also can have well-defined margins.[3] Lipoblastomas can have predominantly low to intermediate signal intensity on T1-weighted sequences and high signal intensity on T2-weighted sequences,[57] predominantly fat signal intensity with an associated cyst,[26] or signal equivalent to fat on all sequences.

Varying amounts of fatty tissue are seen in liposarcomas. The more differentiated liposarcomas have more fat-like tissue, whereas very high-grade tumors often contain no fat at all.[45] Lipomas, liposarcomas,[20] and lipoblastomas all can contain enhancing fibrous septa. Therefore, it is only when a purely fatty tumor has well-defined margins and no areas of internal septation or apparent muscle invasion that the diagnosis of lipoma can be made on MR imaging.[32] In the remaining cases, all three fatty tumors must be included in the differential diagnosis, with liposarcoma being least likely owing to its extreme rarity in children.

Fibromatosis

Fibromatosis can occur in young children, but usually presents in young adults between puberty and 40 years of age. These lesions are characterized by the proliferation of benign fibrosis tissue and have been categorized into superficial and deep groups by Enzinger.[11] When superficial, these tumors are usually small and slow growing. Deep lesions include extraabdominal desmoids, often referred to as *aggressive fibromatosis*,[12] which are typically more aggressive and grow faster.[27]

Fibromatosis is locally aggressive, but never metastasizes.[27] Lesions usually are solitary, but may be multicentric.[27] Involvement of the adjacent neurovascular structures is not unusual.[17] Children with these tumors have variable and unpredictable clinical courses. Treatment includes surgery, radiation therapy, and chemotherapy. Owing to the aggressive nature of this disease, however, recurrence occurs in up to 50% of patients and was reported in seven of eight children in one series.[53]

Fibromatosis has a variable MR imaging appearance (Fig. 12). Lesions can be nodular with well-defined margins or infiltrative with irregular margins or permeation.[53] Some lesions have low signal intensity on T1- and T2-weighted sequences,[12] as would intuitively be expected by the fibrous nature of the lesion. A greater percentage of lesions, however, are of heterogeneous signal intensity with areas of high signal intensity on T2-weighted sequences.[12, 27, 46] Lesions also can have high signal intensity on T1- and T2-weighted sequences.[1] Following gadolinium injection, lesions may enhance diffusely, heterogeneously, or not at all and there is no relationship between the enhancement pattern and patient clinical course.[53]

MR imaging characteristics reflect tumor histology. Lesions with low signal intensity on T2-weighted sequences have a larger collagenous component,[31] whereas tumors with more cellular tissue and less collagen have higher signal intensity on T2-weighted sequences.[27,31] In addition, tumors with

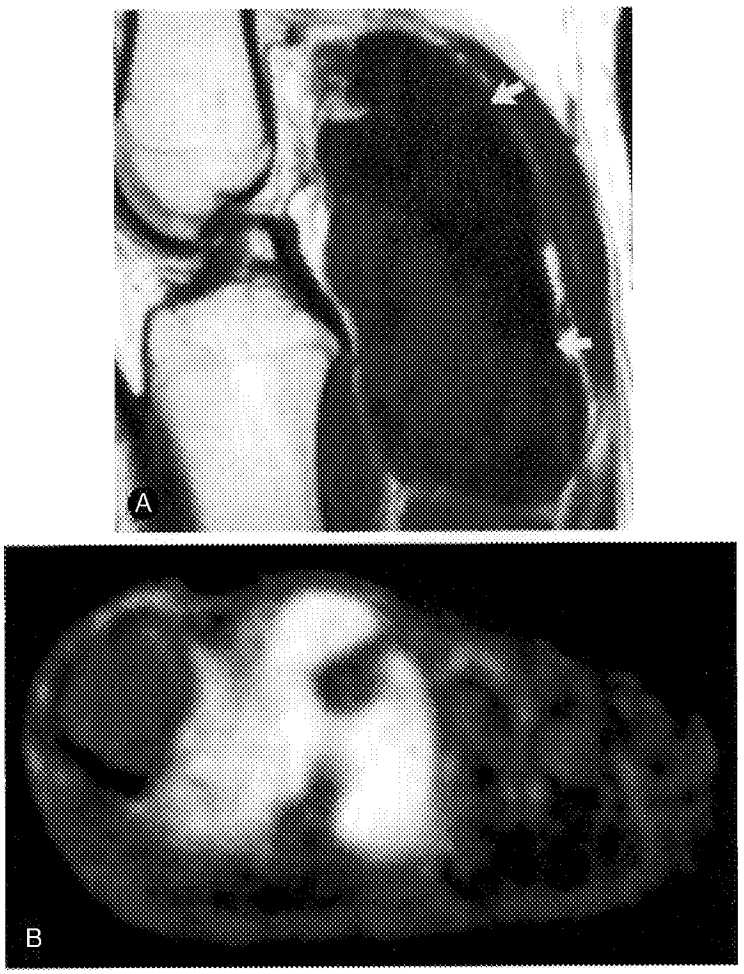

Figure 12. Fibromatosis. *A*, Sagittal T1-weighted image shows mixed intermediate and low signal intensity mass (*arrows*) in the popliteal fossa of this 18-year-old boy. *B*, Axial proton density-weighted image with fat saturation shows high signal intensity mass surrounding the second metatarsal bone in this 4-year-old boy.

high signal intensity on T1-weighted sequences have been found to contain fat or myxoid material.[50]

Neurofibroma

Neurofibromas are the most common benign tumor of the peripheral nerves and may occur as isolated lesions or in association with neurofibromatosis type 1.[6] These tumors are usually sharply defined round or ovoid masses less than 5 cm in diameter.[7]

Neurofibromas have a characteristic target appearance with a central zone of low intensity surrounded by a peripheral zone of higher intensity on T2-weighted images.[7] This target sign also has been seen in schwannomas and multiple target signs have been seen in plexiform neurofibromas.[6] Target signs also may be seen in malignant nerve sheath tumors, but the absence of this sign in the largest component of these tumors appears to be a predictor of malignancy.[6]

Myositis Ossificans

Myositis ossificans is a benign, solitary, ossifying soft-tissue mass that typically occurs in muscle. These tumors are assumed to be posttraumatic, although a history of trauma is not always present.[28] The lesions begin as amorphous soft-tissue masses and slowly mature into well-defined calcified tumors. Children who present with these masses can represent a diagnostic dilemma, especially when a history and other signs of trauma are absent.

On MR imaging, these lesions may simulate a soft-tissue sarcoma.[28, 55] The MR imaging findings of myositis ossificans, however, follow a pattern

related to lesion maturity. Early lesions may have heterogeneous signal intensity with surrounding edema[28] or can have homogeneous internal signal intensity.[55] Intermediate lesions generally are heterogeneous with increased signal intensity and extensive surrounding edema on T2-weighted sequences. Late lesions are well-defined heterogeneous masses with signal approximating fat on T1- and T2-weighted sequences.[28] The CT appearance of these lesions is well described. On CT, a rim of mineralization can be seen around the lesion after 4 to 6 weeks. This rim is much less apparent on MR imaging.[28]

When this entity is suspected plain radiography is performed; CT is preferred over MR imaging. Lesions are prone to recur when surgery is performed prior to lesional maturation, and therefore a reliable diagnosis that avoids biopsy and surgery can improve the patient's clinical course.

Selected Malignant Soft-Tissue Tumors

Soft-Tissue Sarcomas

Soft-tissue sarcomas develop from mesenchymal stem cells and compose 10% to 15% of malignant tumors in children.[60] These tumors have nonspecific MR imaging appearances. Typically, they are of predominantly low signal intensity on T1-weighted and high signal intensity on T2-weighted images, but they can have homogeneous or heterogeneous signal intensity with well- or ill-defined margins on all imaging sequences. Histologic diagnosis requires biopsy.

More than half of soft-tissue sarcomas in children are rhabdomyosarcomas (Fig. 13).[60] These tumors are thought to arise from progenitor cells for striated muscle,[10] but can arise anywhere in the body, even in areas with no striated muscle.[60] The head, neck, genitourinary tract, and extremities are the most common locations.[58] There are three histologic subtypes: embryonal, alveolar, and pleomorphic.[58] The embryonal type is common from birth to 15 years of age[58] and usually is seen in the head, neck, and genitourinary tract.[52] The alveolar type is common between 10 and 25 years of age.[58] Most extremity rhabdomyosarcomas are the alveolar type,[9] which has a poorer prognosis than the embryonal subtype.[52]

The remaining soft-tissue sarcomas are referred to as *nonrhabdomyosarcoma soft-tissue sarcomas* (NRSTS) and consist of a heterogeneous collection of histologic subtypes (Fig. 14*A*). Synovial cell sarcoma is the most common NRSTS in children and composes about 10% of pediatric soft-tissue sarcomas.[60]

Synovial cell sarcoma (see Fig. 14*B*) is extremely rare in children younger than 5 years of age,[60] but 31% occur in patients less than 20 years of age.[42] These tumors develop from mesenchymal cells that differentiate sufficiently to resemble synovial membrane. They frequently occur close to joints, tendons, and bursae, but rarely arise from the intraarticular synovial lining.[43] Synovial cell sarcomas frequently invade, erode, or touch the adjacent

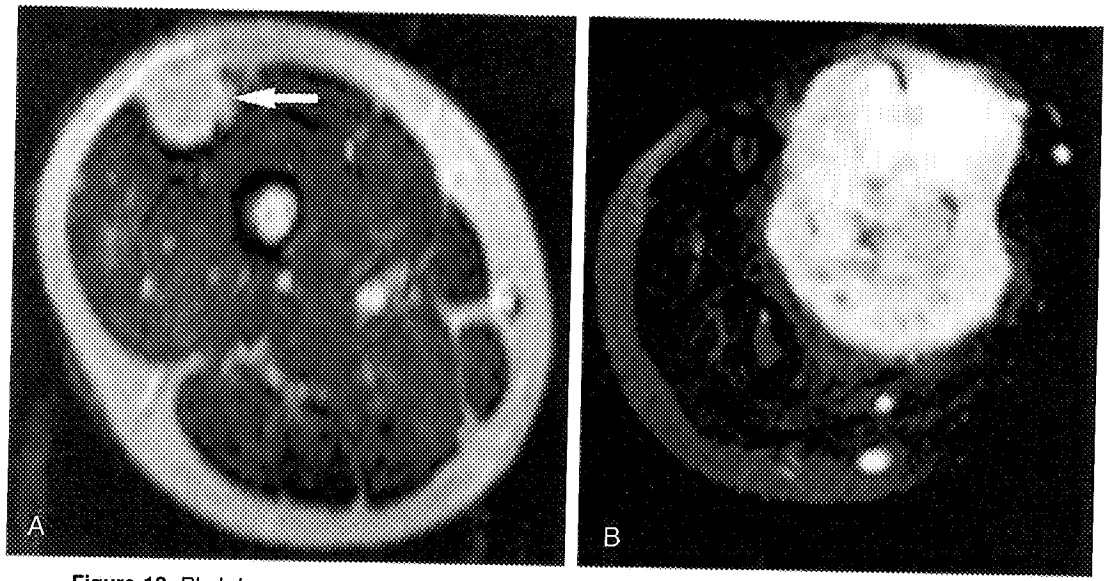

Figure 13. Rhabdomyosarcoma. *A*, Axial T2-weighted image shows a small, fairly well-defined soft-tissue mass (*arrow*) in the thigh of a 15-year-old girl with alveolar type rhabdomyosarcoma. *B*, Axial T2-weighted image with fat saturation shows a large, well-defined soft-tissue mass of heterogeneous signal intensity in the forearm of this 10-year-old girl with alveolar type rhabdomyosarcoma.

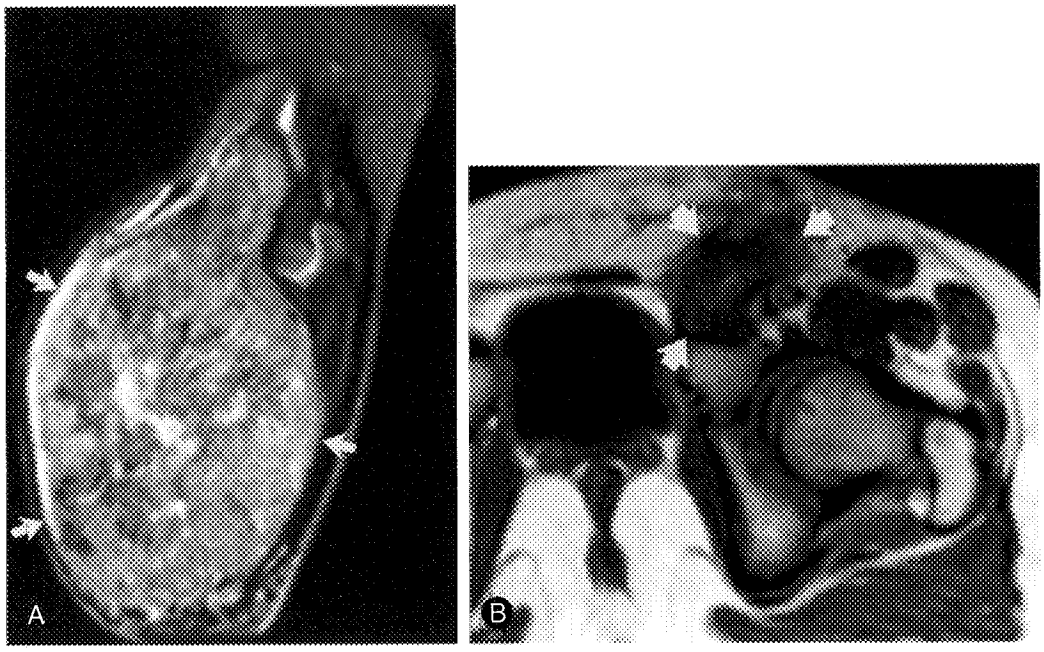

Figure 14. Nonrhabdomyosarcoma soft-tissue sarcomas. *A*, Sagittal T2-weighted image with fat saturation shows large mass (*arrows*) of heterogeneous signal intensity in the forearm of this 2-month-old girl with undifferentiated sarcoma. *B*, Axial T1-weighted image shows mixed low and intermediate signal intensity mass (*arrows*) in this 8-year-old girl with synovial cell sarcoma in the left inguinal region.

bone.[24] Punctate calcifications are seen on plain radiographs in up to 30% of tumors.[43] In addition to the nonspecific MR imaging characteristics already described, synovial cell sarcomas may contain areas of high signal intensity on T1-weighted sequences and fluid-fluid levels that reflect hemorrhage.[24, 43] In the appropriate clinical setting, these MR imaging findings suggest the diagnosis.

Fibrosarcoma is the next most common NRSTS and comprises about 6% of pediatric soft tissue sarcomas.[60] Fibrosarcoma has a congenital form that usually presents in infants and children less than 5 years of age and in children 10 to 15 years of age.[42] Other NRSTS include neurofibrosarcoma, which causes 5% to 10% of NRSTS and occurs in up to 15% of children with von Recklinghausen's disease,[9] and malignant fibrous histiocytoma, which is the most common soft-tissue sarcoma in adults, but is rare in children.[60]

Langerhans Cell Histiocytosis

LCH is a poorly understood disease that is characterized by the accumulation of pathologic Langerhans-like cells, a type of histiocyte. Historically, this disease was termed *eosinophilic granuloma, Hand-Schüller-Christian disease,* or *Letterer-Siwe disease* depending on the patients' signs and symptoms. This disease can involve virtually any organ system in the body and may present with bone lesions or soft-tissue masses.[34]

The radiographic appearance of bone lesions in LCH varies with the area involved and phase of disease. Lesions usually destroy bone and have radiographic features that simulate either benign or malignant disease. Bone lesions usually have low signal intensity on T1-weighted images and high signal intensity on T2-weighted sequences, and appear more extensive than on corresponding plain radiographs.[15] Soft-tissue lesions have a nonspecific MR imaging appearance (Fig. 15) and may or may not be associated with bone involvement.

CONCLUSION

MR imaging plays a major role in the evaluation of children with musculoskeletal masses. MR imaging can confirm the presence, define the location, and characterize soft-tissue masses, occasionally resulting in a specific diagnosis. Plain radiographs are more valuable for determining the specific diagnosis of a bone lesion, but MR imaging is crucial for evaluating the extent of disease and planning surgical intervention.

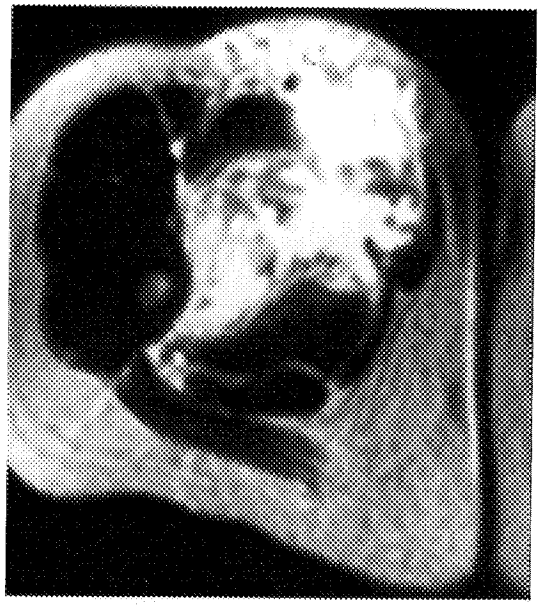

Figure 15. Axial T2-weighted image shows extensive high signal intensity mass with poorly defined margins as the only evidence of disease in this girl with Langerhans cell histiocytosis.

References

1. Ackman JB, Whitman GJ, Chew FS: Aggressive fibromatosis. AJR Am J Roentgenol 163:544, 1994
2. Albright F, Butler AM, Hampton AO, et al: Syndrome characterized by osteitis fibrosa disseminata, areas of pigmentation and endocrine dysfunction, with precocious puberty in females. Report of five cases. New Engl J Med 216:727–746, 1937
3. Arkun R, Memis A, Akalin T, et al: Liposarcoma of soft tissue: MRI findings with pathologic correlation. Skeletal Radiol 26:167–172, 1997
4. Assoun J, Richardi G, Railhac J, et al: Osteoid osteoma: MR imaging versus CT. Radiology 191:217–223, 1994
5. Beltran J, Simon DC, Levy M, et al: Aneurysmal bone cysts: MR imaging at 1.5T. Radiology 158:689–690, 1986
6. Bhargava R, Parham DM, Lasater OE, et al: MR imaging differentiation of benign and malignant peripheral nerve sheath tumors: Use of the target sign. Pediatr Radiol 27:124–129, 1997
7. Bisset GS: MR imaging of soft-tissue masses in children. Magn Reson Imaging Clin North Am 4:697–719, 1996
8. Chung EB, Enzinger FM: Benign lipoblastomatosis: An analysis of 35 cases. Cancer 32:482–492, 1973
9. Cohen MD: Imaging of Children with Cancer. St. Louis, Mosby Year Book, 1992
10. Crist WM, Kun LE: Common solid tumors of childhood. New Engl J Med 324:461–471, 1991
11. Enzinger FM, Weiss SW: Fibromatoses. *In* Soft Tissue Tumors. St. Louis, CV Mosby, 1988, p 136
12. Feld R, Burk DL, McCue P, et al: MRI of aggressive fibromatosis: Frequent appearance of high signal intensity on T2 weighted images. Magn Reson Imag 8:583–588, 1990
13. Fletcher BD, Hanna SL: Pediatric musculoskeletal lesions simulating neoplasms. Magn Reson Imaging Clin North Am 4:721–747, 1996
14. Garces P, Romano CC, Vellet AD, et al: Adamantinoma of the tibia: Plain-film, computed tomography and magnetic resonance imaging appearance. Can Assoc Radiol J 45:314–317, 1994
15. George JC, Buckwalter KA, Cohen MD, et al: Langerhans cell histiocytosis of bone: MR imaging. Pediatr Radiol 24:29–32, 1994
16. Hanna SL, Fletcher BD, Kaste SC, et al: Increased confidence of diagnosis of Ewing sarcoma using T2-weighted MR images. Magn Reson Imaging 12:559–568, 1994
17. Hartman TE, Berquist TH, Fetsch JF: MR imaging of extraabdominal desmoids: Differentiation from other neoplasms. AJR Am J Roentgenol 158:581–585, 1992
18. Hicks DG, Gokan T, O'Keefe RJ, et al: Primary lymphoma of bone. Correlation of magnetic resonance imaging features with cytokine production by tumor cells. Cancer 75:973–980, 1995
19. Himelstein BP, Dormans JP: Malignant bone tumors of childhood. Pediatr Clin North Am 43:967–984, 1996
20. Hosono M, Kobayashi H, Fujimoto R, et al: Septum-like structures in lipoma and liposarcoma: MR imaging and pathologic correlation. Skeletal Radiol 26:150–154, 1997
21. Hubbard AM, Markowitz RI, Kimmel B, et al: Sedation for pediatric patients undergoing CT and MRI. J Comput Assist Tomogr 16:3–6, 1992
22. Jaramillo D, Laor T, Gebhardt MC: Pediatric musculoskeletal neoplasms. Evaluation with MR imaging. Magn Reson Imaging Clin North Am 4:749–770, 1996
23. Jelinek JS, Murphey MD, Kransdorf MJ, et al: Parosteal osteosarcoma: Value of MR imaging and CT in the prediction of histologic grade. Radiology 201:837–842, 1996
24. Jones BC, Sundaram M, Kransdorf MJ: Synovial sarcoma: MR imaging findings in 34 patients. AJR Am J Roentgenol 161:827–830, 1993
25. Karasick D, Schweitzer ME, Eschelman DJ: Symptomatic osteochondromas: Imaging features. AJR Am J Roentgenol 168:1507–1512, 1997
26. Katz DS, Merchant N, Beaulieu CF, et al: Lipoblastoma of the thigh: MR appearance. J Comput Assist Tomogr 20:1002–1003, 1996
27. Kransdorf MJ, Jelinek JS, Moser RP, et al: Magnetic resonance appearance of fibromatosis. A report of 14 cases and review of the literature. Skeletal Radiol 19:495–499, 1990
28. Kransdorf MJ, Meis JM, Jelinek JS: Myositis ossificans: MR appearance with radiologic-pathologic correlation. AJR Am J Roentgenol 157:1243–1248, 1991
29. Kransdorf MJ, Moser RP, Meis JM, et al: Fat-containing soft-tissue masses of the extremities. Radiographics 11:81–106, 1991
30. Lang P, Honda G, Roberts T, et al: Musculoskeletal neoplasm: Perineoplastic edema versus tumor on dynamic postcontrast MR images with spatial mapping of instantaneous enhancement rates. Radiology 197:831–839, 1995
31. Liu P, Thorner P: MRI of fibromatosis: With pathologic correlation. Pediatr Radiol 22:587–589, 1992
32. Ma LD, Frassica FJ, Scott WW Jr, et al: Differentiation of benign and malignant musculoskeletal tumors: Potential pitfalls with MR imaging. Radiographics 15:349–366, 1995

33. Madewell JE, Ragsdale BD, Sweet DE: Radiologic and pathologic analysis of solitary bone lesions. Part I: Internal margins. Radiol Clin North Am 19:715–748, 1981
34. Meyer JS, Harty MP, Mahboubi S, et al: Langerhans cell histiocytosis: Presentation and evolution of radiologic findings with clinical correlation. Radiographics 15:1135–1146, 1995
35. Mirra JM: Adamantinoma and osteofibrous dysplasia. *In* Mirra JM (ed): Bone Tumors: Clinical, Radiologic, and Pathologic Correlations, vol 2. Philadelphia, Lea & Febiger, 1989
36. Mirra JM: Cysts and cyst-like lesions of bone. *In* Mirra JM (eds): Bone Tumors: Clinical, Radiologic, and Pathologic Correlations, vol 2. Philadelphia, Lea & Febiger, 1989
37. Mirra JM: Intramedullary cartilage- and chondroid-producing tumors. *In* Mirra JM (ed): Bone Tumors: Clinical, Radiologic, and Pathologic correlations, vol 1. Philadelphia, Lea & Febiger, 1989
38. Mirra JM: Lymphoma and lymphoma-like disorders. *In* Mirra JM (ed): Bone Tumors: Clinical, Radiologic, and Pathologic correlations, vol 2. Philadelphia, Lea & Febiger, 1989
39. Mirra JM: Parosteal tumors. *In* Mirra JM (ed): Bone Tumors: Clinical, Radiologic, and Pathologic Correlations, vol 2. Philadelphia, Lea & Febiger, 1989
40. Mirra JM, Gold RH, Piero P: Osseous tumors of intramedullary origin. In Mirra JM (ed): Bone Tumors: Clinical, Radiologic, and Pathologic Correlations, vol 1. Philadelphia, Lea & Febiger, 1989
41. Mirra JM, Picci P: Ewing's sarcoma. *In* Mirra JM (ed): Bone Tumors: Clinical, Radiologic, and Pathologic Correlations, vol 2. Philadelphia, Lea & Febiger, 1989
42. Miser JS, Triche TJ, Pritchard DJ, et al: Ewing's sarcoma and the nonrhabdomyosarcoma soft tissue sarcomas of childhood. *In* Pizzo PA, Poplack DG (eds): Principles and Practice of Pediatric Oncology. Philadelphia, JB Lippincott, 1989
43. Morton MJ, Berquist TH, McLeod RA, et al: MR imaging of synovial sarcoma. AJR Am J Roentgenol 156:337–340, 1991
44. Mueller DL, Grant RM, Riding MD, et al: Cortical saucerization: An unusual imaging finding of Ewing Sarcoma. AJR Am J Roentgenol 163:401–403, 1994
45. Munk PL, Lee MJ, Janzen DL, et al: Lipoma and liposarcoma: Evaluation using CT and MR imaging. AJR Am J Roentgenol 169:589–594, 1997
46. O'Keefe F, Kim EE, Wallace S: Magnetic resonance imaging in aggressive fibromatosis. Clin Radiol 42:170–173, 1990
47. Onikul E, Fletcher BD, Parham DM, et al: Accuracy of MR imaging for estimating intraosseous extent of osteosarcoma. AJR Am J Roentgenol 167:1211–1215, 1996
48. Oxtoby JW, Davies AM: MRI characteristics of chondroblastoma. Clin Radiol 51:22–26, 1996
49. Panuel M, Gentet JC, Scheiner C, et al: Physeal and epiphyseal extent of primary malignant bone tumors in childhood. Correlation of preoperative MRI and the pathologic examination. Pediatr Radiol 23:421–424, 1993
50. Quinn SF, Erickson SJ, Dee PM, et al: MR imaging in fibromatosis: Results in 26 patients with pathologic correlation. AJR Am J Roentgenol 156:539–542, 1991
51. Ragsdale BD, Madewell JE, Sweet DE: Radiologic and pathologic analysis of solitary bone lesions. Part II: periosteal reactions. Radiol Clin North Am 19:749–783, 1981
52. Raney RB Jr, Hays DM, Tefft M, et al: Rhabdomyosarcoma and the undifferentiated sarcomas. *In* Pizzo PA, Poplack DG (eds): Principles and Practice of Pediatric Oncology. Philadelphia, JB Lippincott, 1989, p 640
53. Romero JA, Kim EE, Kim CG, et al: Different biologic features of desmoid tumors in adult and juvenile patients: MR demonstration. J Comput Assist Tomogr 19:782–787, 1995
54. Schima W, Amann G, Stiglbauer R, et al: Preoperative staging of osteosarcoma: Efficacy of MR imaging in detecting joint involvement. AJR Am J Roentgenol 163:1171–1175, 1995
55. Shirkhoda A, Armin AR, Bis KG, et al: MR imaging of myositis ossificans: Variable patterns at different stages. J Magn Reson Imaging 5:287–292, 1995
56. Springfield DS, Rosenberg AE, Mankin HJ, et al: Relationship between osteofibrous dysplasia and adamantinoma. Clin Orthop Rel Res 309:234–244, 1994
57. Schultz E, Rosenblatt R, Mitsudo S, et al: Detection of a deep lipoblastoma by MRI and ultrasound. Pediatr Radiol 23:409–410, 1993
58. Suzuki Y, Ehara S, Shiraishi H, et al: Embryonal rhabdomyosarcoma of foot with expansive growth between metatarsals. Skeletal Radiol 26:128–130, 1997
59. Sweet DE, Madewell JE, Ragsdale BD: Radiologic and pathologic analysis of solitary bone lesions. Part III: matrix patterns. Radiol Clin North Am 19:785–814, 1981
60. Treuner J, Altmannsberger M, Niethammer D: Soft tissue sarcomas. Monogr Paediatr 18:243–263, 1986
61. Tsai JC, Dalinka MK, Fallon MD, et al: Fluid-fluid level: A nonspecific finding in tumors of bone and soft tissue. Radiology 175:779–782, 1990
62. Uri DS, Dalinka MK, Kneeland JB: Muscle impingement: MR imaging of a painful complication of osteochondromas. Skeletal Radiol 25:689–692, 1996
63. Verstraete KL, DeDeene Y, Roels H, et al: Benign and malignant musculoskeletal lesions: Dynamic contrast-enhanced MR imaging parametric first-pass images depict tissue vascularization and perfusion. Radiology 192:835–843, 1994
64. Weatherall PT, Maale GE, Mendelsohn DB, et al: Chondroblastoma: Classic and confusing appearance at MR imaging. Radiology 190:467–474, 1994
65. Yamamura S, Sato K, Sugiura H, et al: Inflammatory reaction in chondroblastoma. Skeletal Radiol 25:371–376, 1996
66. Yao L, Eckardt JJ, Seeger LL: Fibrous dysplasia associated with cortical bony destruction: CT and MR findings. J Comput Assist Tomogr 18:91–94, 1994
67. Youssef BA, Haddad MC, Zahrani A, et al: Osteoid osteoma and osteoblastoma: MRI appearances and the significance of ring enhancement. Eur Radiol 6:291–296, 1996
68. Zehr RJ, Recht MP, Bauer TW: Adamantinoma. Skeletal Radiol 24:553–555, 1995

Address reprint requests to

James S. Meyer, MD
Department of Radiology
Children's Hospital of Philadelphia
34th St. and Civic Center Blvd.
Philadelphia, PA 19104